Exploring the Cramer-Lundberg Model: Time Grid Simulations, SDE Approximations, & Ruin Probability Estimates

Kavesh Biersay, Justin Wu, Elsa Tcheuyap

December 5, 2024

Abstract

This report introduces the Cramer-Lundberg Model, and investigates its history, uses, and drawbacks. Jump-times only and fixed time grid simulations are plotted and analyzed for various values of model parameters; we find that fixed-time grid simulations generally lead to a wider spread of sample paths. An SDE approximation to the model is introduced, and found to take slightly higher values than the fixed-grid simulation on the interval $[0, 5]$*. Estimation methods for ruin probabilities are investigated on* $[0, 5]$*, leading to a sample mean estimate of 0.1512, and a control variate estimate of 0.1575 (with 43% lower associated variance). For an infinite interval* $[0, \infty)$*, claim-sizes are assumed to be Exponential*(1)*, leading to an importance sampling estimate of* 2.26617×10^{-5} for the ultimate ruin probability.

1 Report Outline and Goals

This report covers the following topics:

- In Section 2, we introduce the Cramer-Lundberg Model, and describe its history, uses, and drawbacks.
- In Section 3, we define specific values for the parameters of the model; these values are used in Sections 4-5, and Section 6.1-6.2. (Note that we use a different set of values in Section 6.3 of this report; our reasoning is explained in that section).
- In Section 4, we simulate the model through two approaches: (i) by only simulating its behaviour at time points where claims occur, and (ii) by simulating its behaviour on a fixed time grid with discrete spacings of equal lengths. We investigate how adjusting specific parameters of the model affects the outputs of these simulations.
- In Section 5, we introduce a stochastic differential equation (SDE) that can approximate the model, and compare simulations of this SDE with simulations of the model on the fixed time grid.
- In Section 6, we introduce the mathematical definition of ruin probability, and implement several methods for estimating ruin probabilities over finite and infinite time intervals. Specifically, we compute sample mean and control variate estimators for the ruin probability on a finite interval $[0, T]$, and compute an importance sampling estimator for the ruin probability on an infinite interval $[0, \infty)$.
- In Section 7, we summarize key results that were obtained in this report, and discuss the limitations of our approaches in Sections 4-6, as well as next steps for improving upon our work in those sections.

2 Introducing the Cramer-Lundberg Model

The Cramer-Lundberg model is a famous model in actuarial science that describes the wealth process of an insurance company. It is defined by the equation:

$$X_t = x + ct - \sum_{i=1}^{N_t} Y_i \tag{1}$$

where $c > 0$ is the insurance company's premium, N_t is a Poisson process with rate $\lambda > 0$ which represents the number of claims paid out by the company up to time t, and Y_i are i.i.d. random variables which represent the respective claim sizes to be paid to the policyholders of the insurance company.

This model assumes that the company can only gain wealth by the premium rate c, and the only way the company can lose wealth is through claims Y made by its clients.

2.1 History of the Model

The basic insurance risk model goes back to the early work by Filip Lundberg who in his famous Uppsala thesis of 1903 laid the foundation of actuarial risk theory. Lundberg realised that Poisson processes lie at the heart of non–life insurance models. Via a suitable time transformation (so–called operational time) he was able to restrict his analysis to the homogeneous Poisson process. This "discovery" is similar to the recognition by Bachelier in 1900 that Brownian motion is the key building block for financial models. It was then left to Harald Cramer and his Stockholm School to incorporate Lundberg's ideas into the emerging theory of stochastic processes. In doing so, Cramer contributed considerably to laying the foundation of both non–life insurance mathematics as well as probability theory.

2.2 Uses of the Cramer-Lundberg Model

There are several uses of the Cramer-Lundberg Model in Actuarial Science. These include:

- Ruin Probability Estimation: to estimate the likelihood that the insurer's wealth becomes negative over time.
- Risk Management: to ensure an insurer can cover its liabilities (in this case claims).
- Premium Setting: to allow for the calculation of premiums to maintain a certain wealth target.
- Aggregate Claims Distributions: to help in calculating the distributions of aggregate claims over time. (Aggregate claims refers to sum of claims that the company has to pay out and together these claims may follow a certain distribution)

2.3 Drawbacks of the Cramer-Lundberg Model

There are several drawbacks of using the Cramer-Lundberg Model as a means of valuing the wealth process of an insurance company. These include:

- The model does not account for premium payments that are periodic. It assumes a constant premium rate over time.
- It does not account for investment income from the company's reserves or any other cash flows the company may have. (Assumes only cash flows are constant premium and claims)
- It assumes claim amounts are independent, which may not be the case in practice.
- It assumes the probability of extreme claim sizes is rare, which may not be the case in practice.

3 Setting the Parameters of the Model

3.1 Setting the Parameters of the Model

For this project, we set the parameters of the model to be the following values:

- $x = 10$
- $c = 4.4$
- $\lambda = 2$
- $Y \sim Gamma(k = 2, \theta = 1)$

In this project, we have also assumed that $c = (1+\eta)\lambda\mathbb{E}[Y]$ where η is the safety loading factor. The safety loading factor ensures that the insurer has sufficient funds to cover claims even in adverse scenarios. In this case, we have set $\eta = 0.1$.

Note that all graphs and outputs are based on these parameters, unless otherwise specified.

3.2 Python Code Attachment

All code written for this report is attached to this submission as a Python Notebook file. When we refer to this Notebook file in subsequent sections of the report this, we will simply call it the 'Notebook'.

4 Simulations of the Cramer Lundberg Model

In this section, we simulate the Cramer-Lundberg Model through two approaches: (i) simulating exclusively the time-points at which a jump (i.e. claim) occurs, and (ii) simulating the values of the model at Ndt time points on a fixed time grid.

For both methods, we simulate the model over a finite time interval $[0, T]$, with $T = 5$.

4.1 Simulating the Cramer-Lundberg Model Using Jump Times Only

The first of two ways the process can be simulated is by simulating the jump times. This simulations plots the evolution of the wealth process as a step function. The plot below illustrates increases caused by the premium income followed by sharp falls caused by claims. The frequency of the claims follows a Poisson distribution, and the size of the claims follow a Gamma distribution as required by the model.

In this simulation the jump times represent moments where the claims occur which are uniformly distributed within the interval and sorted in chronological order as per the algorithm described in [CT04]. The premium income is calculated for each jump time as being the accumulation of income over time. The corresponding claim sizes were then sampled from the Gamma distribution, and the wealth is updated at each jump time, resulting in a plot displaying the evolution of these values over time.

The uniform distribution of jump times introduces variability in the paths taken by the wealth process as seen in the plot provided. The number of jumps produces additional impact on the simulation as well. A higher number of jumps results in increased frequency of claims, which leads to a more rapid depletion of wealth. Conversely, fewer jumps allow the wealth to grow steadily as premium income accumulates.

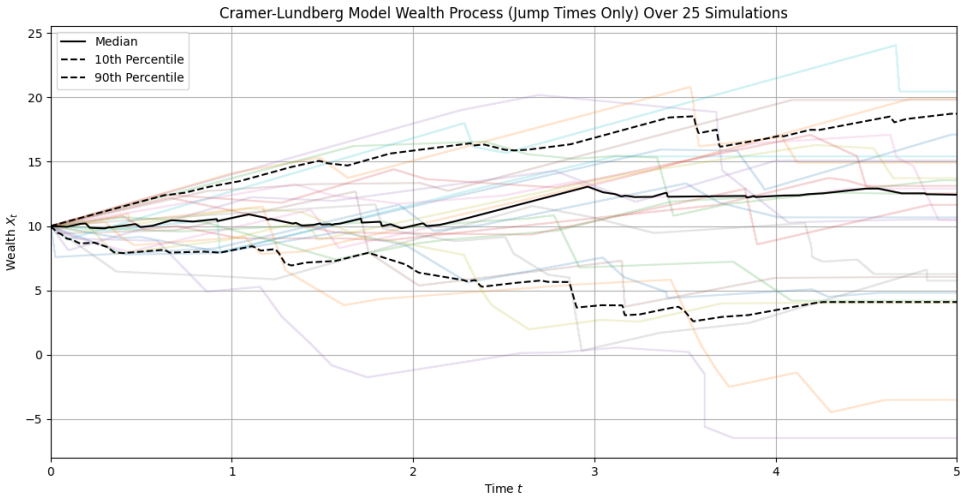

Figure 1: Cramer-Lundberg Model Simulation using Jump Times Only

4.2 Simulating the Cramer-Lundberg Model using a Fixed Time Grid

While the jump-times plot gives data of the values of the wealth process at each jump on $[0, T]$, we can gain a clearer picture of the model's behaviour at a larger number of equidistant time points, by implementing the following algorithm described in [CT04]:

- Split the interval $[0, T]$ into Ndt intervals, with corresponding endpoints $t_1, ..., t_n$.
- Simulate n independent Gaussian random variables $G_i \sim \mathcal{N}(0, (t_i - t_{i-1})\sigma^2)$.
- Simulate the compound Poisson part, exactly as done in Section 4.1.

The discretized trajectory of a sample path generated using this algorithm will then be given by

$$X_{t_i} = x + ct_i + \sum_{k=1}^{i} G_k - \sum_{j=1}^{N_T} Y_{j,t_j} \mathbf{1}_{t_j \leq t_i}, \tag{2}$$

where Y_{j,t_j} represents the jth claim, which arrives at time t_j on the interval $[0, T]$.

Our implementation of this algorithm in Python is contained in the Notebook. We set $Ndt = 1000$ and generate a sample of $N = 100$ simulations; a few sample paths are plotted below, along with the median, 10th percentile, and 90th percentile paths of the entire sample (ranked in terms of their final surplus value):

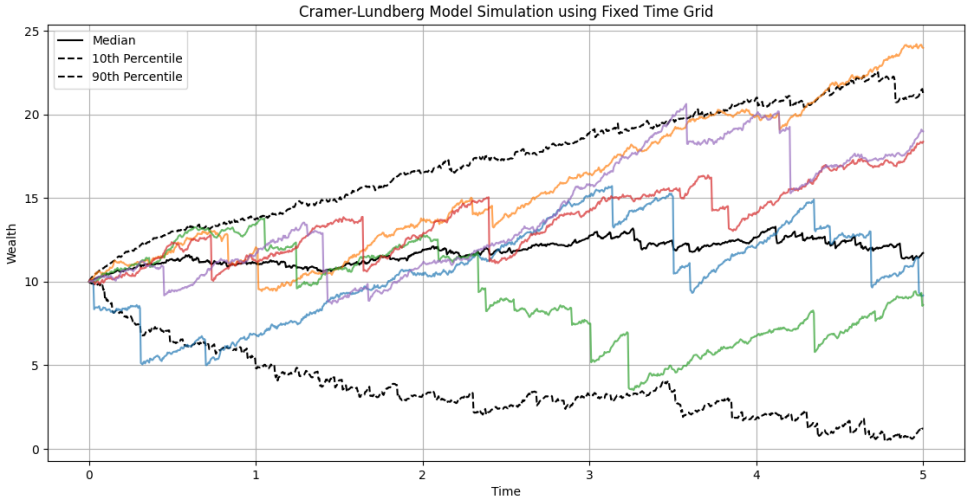

Figure 2: Cramer-Lundberg Model Simulation using a Fixed Time Grid

Comparing this plot to our plot in Section 4.1 for simulating the model using jump-times only, we see that the range of paths in the latter plot appears to be wider than the plot in Section 4.1. This is likely due to the effect of the Gaussian random variable $G_i \sim \mathcal{N}(0, (t_i - t_{i-1})\sigma^2)$, which introduces a wider spread in the final surplus of the sample paths due to its positive variance term.

4.3 Effects of Adjusting the Fixed Time Grid Algorithm Parameters

We will now investigate the effect of changing each individual parameter of the algorithm defined in Section 4.2, while leaving the other parameters fixed with the values given to them in Section 3. Specifically, we will use Python plots to visualize the effects of changing the parameters c, σ, λ, k, θ, and Ndt; in addition, we will provide an analysis of these plots and offer reasons for why certain patterns are present in the data.

Note that in each specific plot of the following subsections, we performed $N = 50$ simulations to gain a comprehensive picture of the overall trends arising from changes to each parameter.

4.3.1 Effects of Changing the Premium Rate c

Plots of the fixed time grid algorithm given different input values of the premium rate, c, are shown below.

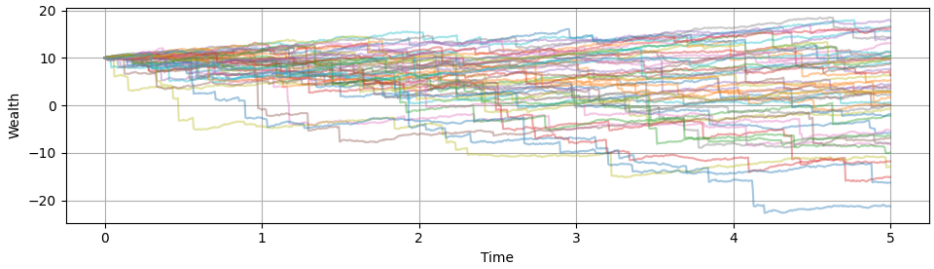

(a) c = 2.2

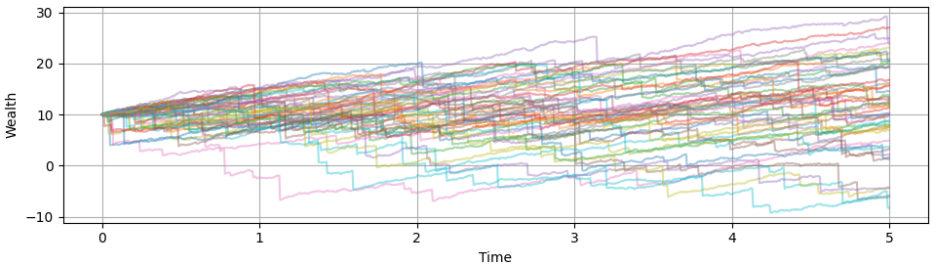

(b) c = 4.4

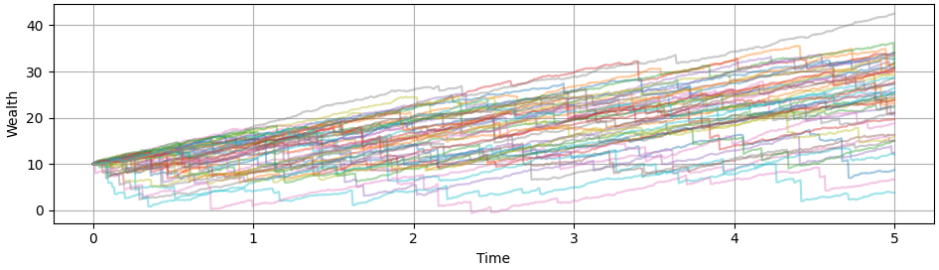

(c) c = 6.6

Explanation of Plots: The Premium Rate c represents the income of the insurance company. Therefore, we would expect that as c increases, the wealth of the company would increase. In the plots, this is reflected by a gradual upward trend in the average rate of increase of sample paths, as c is increased.

4.3.2 Effects of Adjusting the Volatility σ

Plots of the fixed time grid algorithm given different input values of the volatility, σ, are shown below.

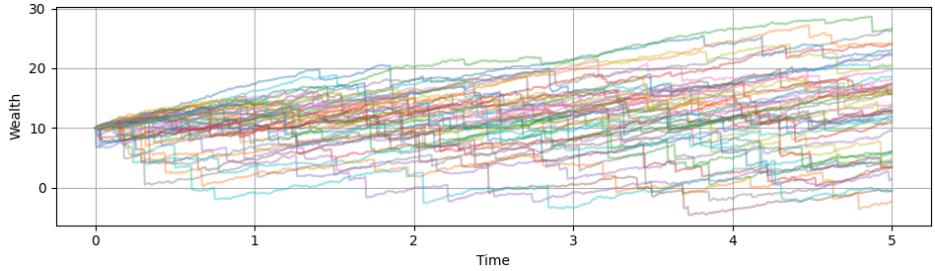

(d) $\sigma = 1$

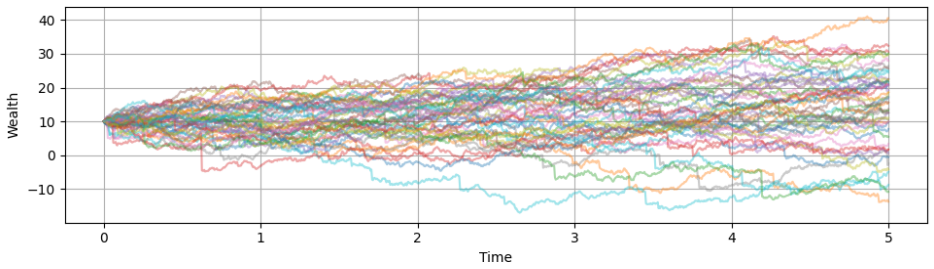

(e) $\sigma = 4$

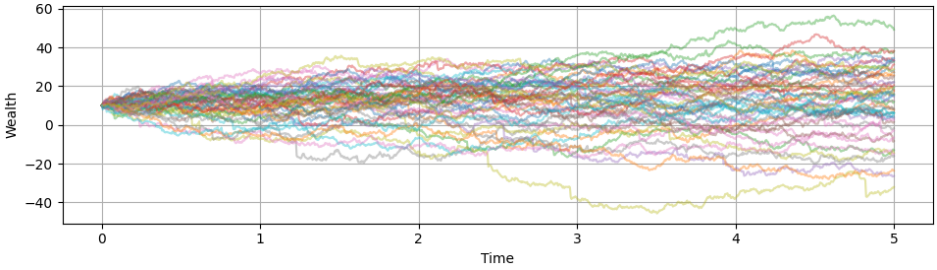

(f) $\sigma = 7$

Explanation of Plots: The Volatility σ is a term in the Gaussian random variable $G_i \sim \mathcal{N}(0, (t_i - t_{i-1})\sigma^2)$; this random variable induces a random movement up or down at each time-point on the time grid. With higher σ, the variance of G_i will increase and hence will cause the behaviour of the sample paths to become more erratic, which suggests that we should see a wider spread in the final surplus of sample paths—in other words, we should expect to see more paths with higher net profits, but also more paths with greater net losses. Indeed, this is reflected by the behaviour of the plots, as the range of paths in plot (d) is around 0-30, while the range of paths in plot (f) is around -40-60.

4.3.3 Effects of Adjusting the Claim Jump Intensity λ

Plots of the fixed time grid algorithm given different input values of the claim jump intensity, λ, are shown below.

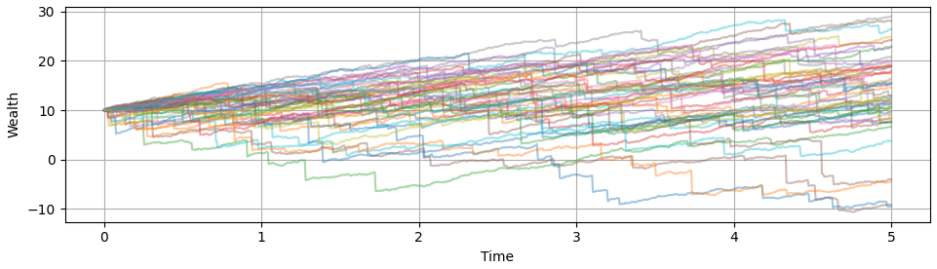

(g) $\lambda = 2$

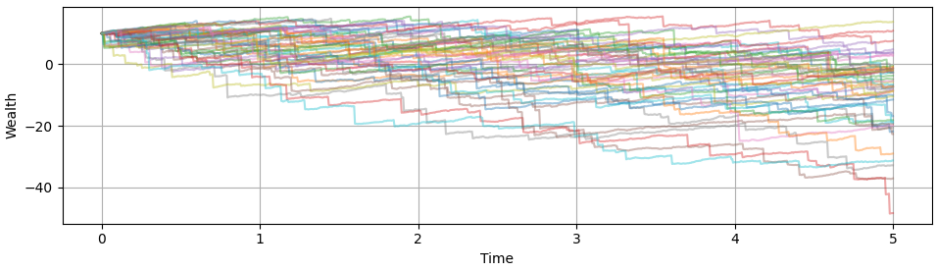

(h) $\lambda = 4$

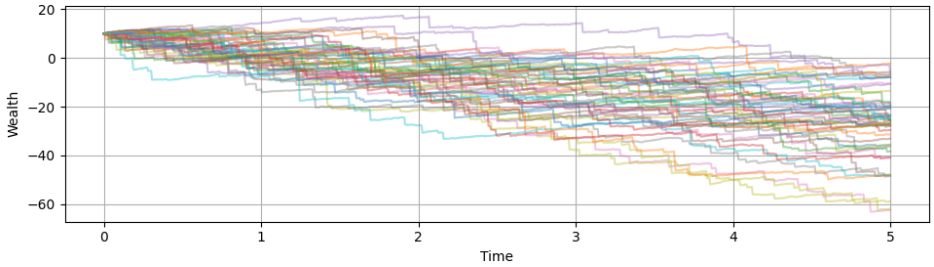

(i) $\lambda = 6$

Explanation of Plots: The Lambda λ represents the average number of claims arriving per unit time. Therefore, we would expect that as λ increases, the average number of claims we receive per unit time would also increase and our wealth would decrease. In our plots, this is highlighted by a downward trend as λ increases: plot (g) has paths generally moving slightly upward, while plots (h) and (i) have paths generally moving downward; plot (i) has the most drastic downward movement and the highest value of λ. Furthermore, there appears to be a higher average number of jumps present in the paths in plot (i), and a lower average number of jumps in the paths in plot (g).

4.3.4 Effects of Adjusting the Shape Parameter k of the Gamma-Distributed Claim Sizes Y_i

Plots of the fixed time grid algorithm, given different input values of the shape parameter k of the Gamma-Distributed claims, are shown below.

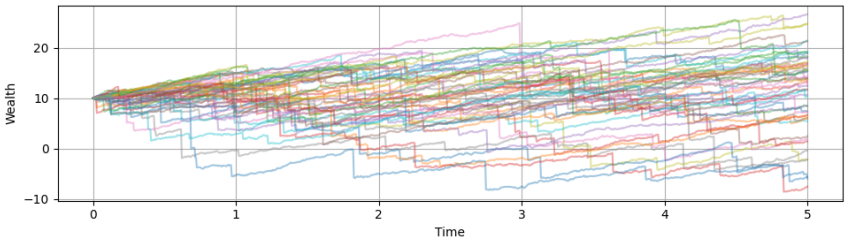

(j) $k = 2$

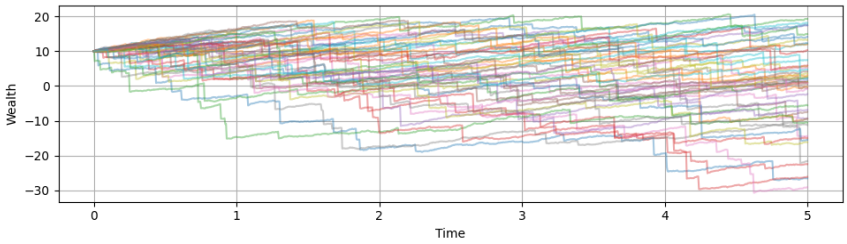

(k) $k = 3$

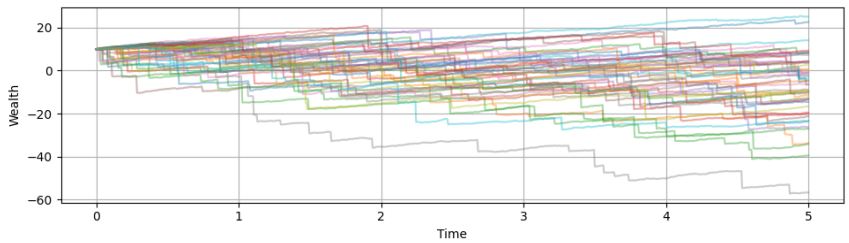

(l) $k = 4$

Explanation of Plots: The Shape k represents the shape parameter of the claim-size Gamma distribution. Since $\mathbb{E}[Y] = k\theta$ when $Y \sim Gamma(k, \theta)$, we would expect that as k increases, the claim sizes will also generally increase, leading to lower wealth. In our plots, this is highlighted by a downward trend as k increases: plot (j) has paths generally moving slightly upward, while plots (k) and (l) have paths generally moving downward; plot (l) has the most drastic downward movement and the highest value of k.

4.3.5 Effects of Adjusting the Scale Parameter θ of the Gamma-Distributed Claim Sizes Y_i

Plots of the fixed time grid algorithm, given different input values of the scale parameter θ of the Gamma-Distributed claims, are shown below.

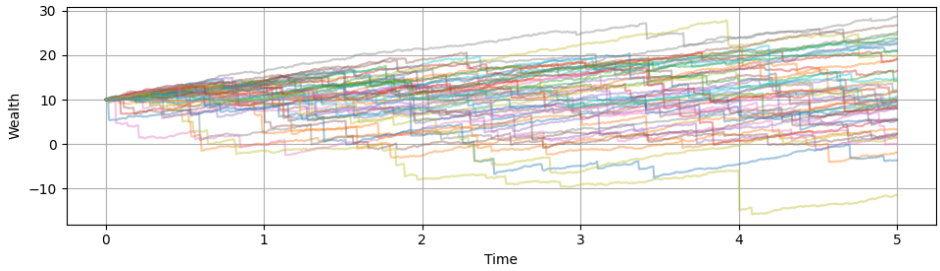

(m) $\theta = 1$

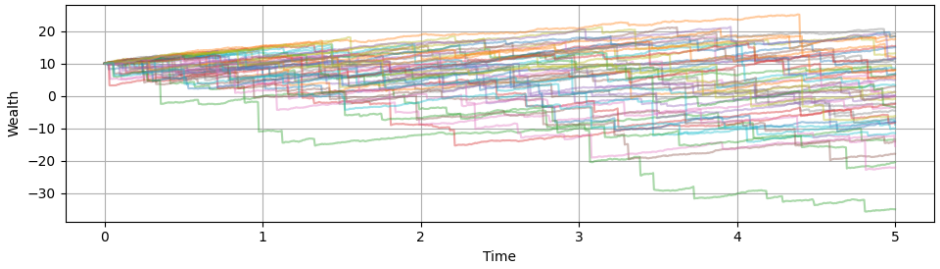

(n) $\theta = 1.5$

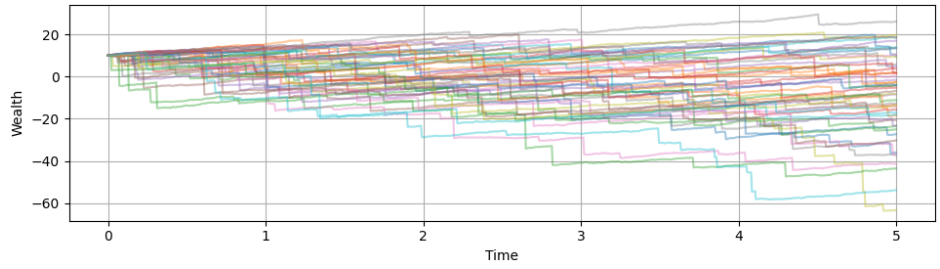

(o) $\theta = 2$

Explanation of Plots: The Scale θ represents the scale parameter of the claim-size Gamma distribution. Since $\mathbb{E}[Y] = k\theta$ when $Y \sim Gamma(k, \theta)$, we would expect that as θ increases, the claim sizes will also generally increase, leading to lower wealth. In our plots, this is highlighted by a downward trend as θ increases: plot (m) has paths generally moving slightly upward, while plots (n) and (o) have paths generally moving downward; plot (o) has the most drastic downward movement and the highest value of θ.

4.3.6 Effects of Adjusting the Number of Time Intervals Ndt on the Fixed Time Grid

Outputs of the fixed time grid algorithm, given different input values of the number of time intervals Ndt on the fixed time grid, are shown below.

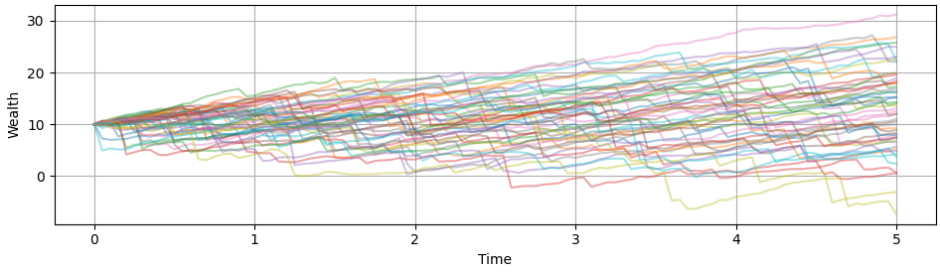

(p) $Ndt = 100$

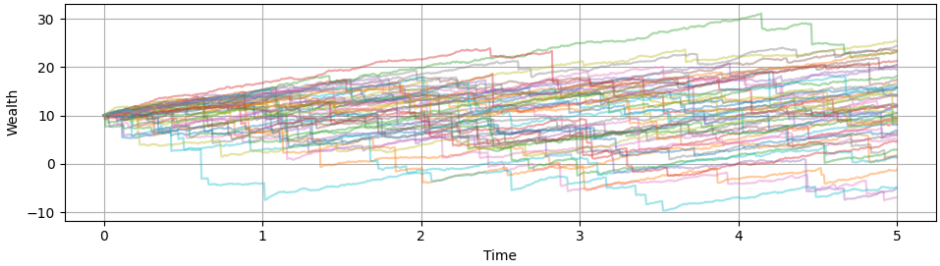

(q) $Ndt = 1000$

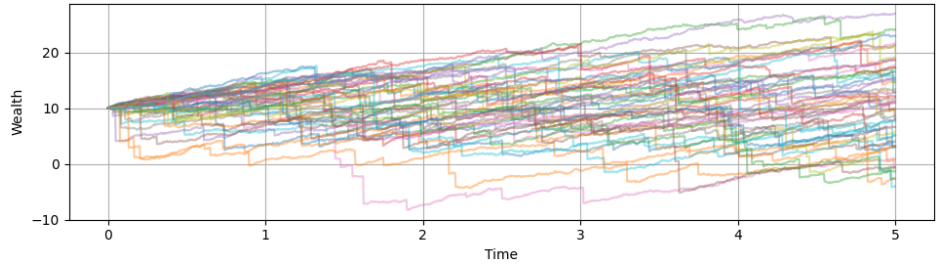

(r) $Ndt = 2000$

Explanation of Plots: The Number of Time Intervals Ndt represents the number of time intervals that are included in the respective plot—when Ndt is larger, there are more intervals of time on the grid. However, since the overall time of simulation is capped at $T = 5$, this means that the length of time of each interval decreases, causing the plots to look rougher and more jagged. Indeed, this is shown through the above plots, where we can see the difference between plot (p) where the paths are relatively smoother, and plot (r) where the paths are more jagged.

5 SDE Approximation of the Cramer-Lundberg Model

5.1 Introducing the Approximation

An SDE approximation to the Cramer-Lundberg model is

$$dX_t = (c - \lambda \mathbb{E}[Y])dt - \sqrt{\lambda \mathbb{E}[Y^2]}dW_t, \tag{3}$$

where W_t is standard Brownian motion. We will implement code which simulates sample paths of this SDE in Python, and compare the results yielded by this code to the results we obtained from our fixed-time grid algorithm in Section 4.2.

5.2 Simulating the Cramer-Lundberg SDE Approximation

Python code which simulates the SDE approximation (3) is contained in the Notebook. For a sample of $N = 100$ simulations, a few sample paths are plotted below, along with the median, 10th percentile, and

90th percentile paths of the entire sample (ranked in terms of their final surplus value).

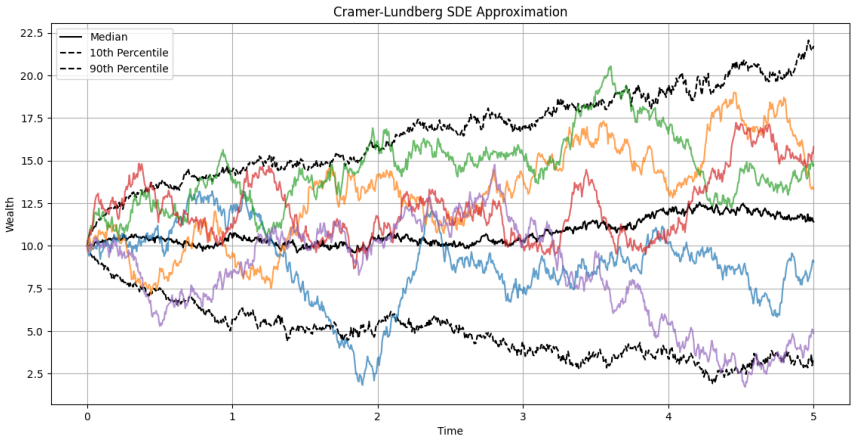

Figure 3: Cramer-Lundberg SDE Approximation Simulation

We can see that sample paths of this SDE approximation are quite jagged. This reflects the inherent discontinuities in the surplus process due to random claim arrivals and sizes.

5.3 Comparing Simulations of the SDE Approximation and Fixed Time Grid

When comparing the simulation to the approximation, the most obvious difference is that the approximation reflects smooth changes over time (as seen in blue on the graph below). In the grid-based approximation, seen in the broken orange line, claims following the Poisson process are illustrated through discrete jumps in the plot.

After adjusting the parameters repeatedly, it was found that a higher loading factor (η) resulted in closer proximity between the simulation and approximation. In particular, we consistently observed similar results with both models when setting $\eta = 0.9$.

The parameters for which the simulation followed the approximation most closely were $\lambda = 5$, lambda set $k = 2$, $\theta = 1$, and $\eta = 0.9$ as seen below. The two followed quite similar trends for the first two time steps; however the wealth process of the grid-based simulation generally takes slightly lower values than the wealth process of the SDE approximation.

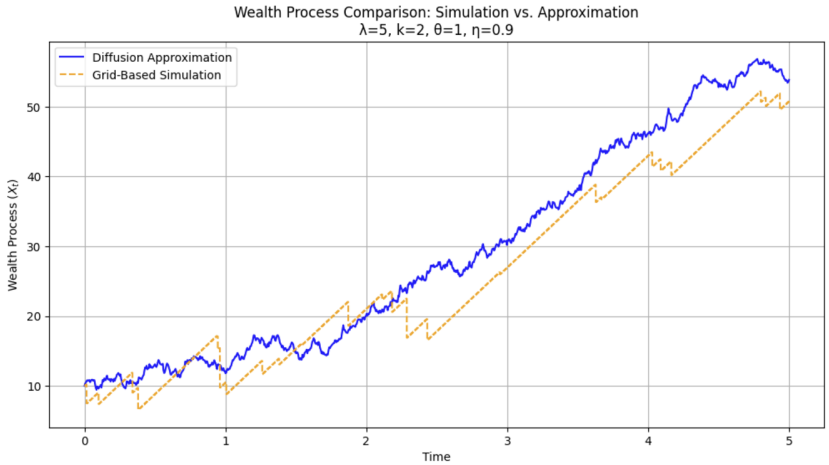

Figure 4: Comparing Grid-based Simulation to Diffusion Approximation for Wealth Evolution

6 Estimating Ruin Probabilities under the Cramer-Lundberg Model

6.1 Defining Ruin Probability

For a given Cramer-Lundberg wealth process X with initial condition $X_0 = x$, and a given time interval $[0, T]$, we define R to be the indicator random variable

$$R \sim \mathbf{1}_{(\exists t \in [0,T] \text{ s.t. } X_t \leq 0 | X_0 = x)} \tag{4}$$

which takes value 1 if X is ever non-positive on $[0, T]$ (i.e., X represents a wealth process where ruin was achieved by the insurance company), and takes value 0 otherwise. Building on this, we define the *ruin probability* of X on the infinite time interval $[0, \infty)$ as

$$\psi_T(x) = \mathbb{E}[R] = \mathbb{P}(\exists t \in [0, T] \text{ s.t. } X_t \leq 0 | X_0 = x). \tag{5}$$

Similarly, we define U to be the indicator random variable

$$U \sim \mathbf{1}_{(\exists t \in [0,\infty) \text{ s.t. } X_t \leq 0 | X_0 = x)} \tag{6}$$

and define the *ultimate ruin probability* to be

$$\psi_\infty(x) = \mathbb{E}[U] = \mathbb{P}(\exists t \in [0, T] \text{ s.t. } X_t \leq 0 | X_0 = x). \tag{7}$$

6.2 Estimating Ruin Probabilities over a Finite Time Interval $[0, T]$

6.2.1 Sample Mean Estimation of Ruin Probability on $[0, T]$

The definition of ruin probability outlined in (5) suggests that a feasible way to estimate $\psi_T(x)$ would be to compute the average of a large number of independent realizations of R. Specifically, we can define a sample mean estimator for $\psi_T(x)$ as

$$\widehat{\psi_T(x)}_{s.m.} = \frac{1}{N_{sims}} \sum_{i=1}^{N_{sims}} R_i, \tag{8}$$

where R_i is the ith realization of the r.v. R defined in Section 4.2. The Law of Large Numbers says that (8) is a consistent estimator of $\mathbb{E}[R] = \psi_T(x)$; moreover, this estimator is quite feasible to compute, since doing so merely involves simulating a large number N_{sims} of realizations of R and computing the sample mean. As such, we implement code to compute our estimator in Python (this can be found in the Notebook); setting $N_{sims} = 10000$ yields the result of

$$\widehat{\psi_T(x)}_{s.m.} = 0.1512, \tag{9}$$

with associated variance

$$\text{Var}\left(\widehat{\psi_T(x)}_{s.m.}\right) = 1.3264 \times 10^{-5}. \tag{10}$$

6.2.2 Control Variate Estimation of Ruin Probability on $[0,\ T]$

As an extension of our work in Section 4.3.1, we can reduce the variance of our estimate of $\psi_T(x)$ by using the method of control variates. Specifically, by defining the random variable $F = X_T$ to be the final surplus of the wealth process X at time T, we can define a control variate estimator for $\psi_T(x)$ as

$$\widehat{\psi_T(x)}_{c.v.} = \frac{1}{N_{sims}} \sum_{i=1}^{N_{sims}} \psi_T(x) \approx \frac{1}{N_{sims}} \sum_{i=1}^{N_{sims}} [R_i - b^*(F_i - \mathbb{E}[F])] \tag{11}$$

where

$$b^* = \frac{\text{Cov}(R, F)}{\text{Var}(F)} \tag{12}$$

is the constant which ensures that variance minimization is achieved [Gla03], and

$$\mathbb{E}[F] = \mathbb{E}\left[x + cT - \sum_{i=1}^{N_T} Y_i\right] = x + (c - \lambda k\theta)T$$

is the expected value of the final surplus, given the parameters defined in Section 3.1. Note that $\widehat{\psi_T(x)}_{c.v.}$ is a consistent estimator [Gla03], and thus it will converge to the true ruin probability $\psi_T(x)$ as $N_{sims} \to \infty$.

Through our implementation of this method with $N_{sims} = 10000$, we obtain the estimate of

$$\widehat{\psi_T(x)}_{c.v.} = 0.1575, \tag{13}$$

with an associated variance

$$\text{Var}\left(\widehat{\psi_T(x)}_{c.v.}\right) = 7.59264 \times 10^{-6}. \tag{14}$$

This variance is approximately 43% smaller than the value of $\text{Var}\left(\widehat{\psi_T(x)}_{s.m.}\right)$ obtained in (10), which shows that control variate estimation is indeed a valid technique for increasing the precision of our ruin probability estimate. Our code for this part can be found in the Notebook.

6.3 Estimating Ruin Probabilities over an Infinite Time Interval [0,∞)

6.3.1 Defining New Parameters for Ultimate Ruin Probability Estimation

For the remainder of the report, we make the following changes to the parameters of the model:

- *Claim sizes* are now distributed as $Y_i \sim \text{Exponential}(\alpha)$, where $\alpha = 1$.
- The *initial wealth* of the insurer is $x = 20$.
- The *premium rate* is $c = 1$.
- The *number of claims* on $[0, t]$ is now distributed as $N_t \sim \text{Poisson}(\lambda t)$, where $\lambda = 0.5$. In particular, this implies that the *interarrival times between claims* are distributed as $\xi_i \sim \text{Exponential}(\lambda)$.

These changes are done to ensure tractability—in particular, using exponentially distributed claim sizes will greatly simplify the mathematics involved in justifying our approach to estimating $\psi_\infty(x)$. This will enable us to convey the essential elements of the importance sampling technique without getting bogged down in lengthy calculations.

6.3.2 Motivating the Usage of Importance Sampling Estimation

Define the *net gain between successive claim times*, Z_i, as

$$Z_i = c\xi_i - Y_i,$$

where $c\xi_i$ represents the amount gained through premium between the $(i-1)^{th}$ and i^{th} claim, and Y_i represents the amount lost due to the i^{th} claim. Further, define S_n to be the sum of the first n realizations of Z_i:

$$S_n = \sum_{i=1}^{n} Z_i, \tag{15}$$

and define τ_x to be a random variable describing the number of claims up to the point in time where ruin is achieved,

$$\tau_x = \inf\{n : S_n < -x\}. \tag{16}$$

For a wealth process X_t with initial condition $X_0 = x$, [Gla03] gives an equivalent definition of the ultimate ruin probability $\psi_\infty(x)$ as

$$\psi_\infty(x) = \mathbb{P}(\tau_x < \infty \mid X_0 = x). \tag{17}$$

In our model, where our parameters are defined as in Section 4.4.1, the drift of Z_i is

$$\mathbb{E}[Z_i] = \mathbb{E}[c\xi_i] - \mathbb{E}[Y_i] = \frac{c}{\lambda} - \frac{1}{\alpha} = \frac{1}{0.5} - 1 = 2 - 1 > 0, \tag{18}$$

which means that $\mathbb{P}(\tau_x < \infty \mid X_0 = x) < 1$ according to [Gla03], since the expected net gain between successive claims is positive. As such, sampling from the original distribution under the measure $\mathbb{P}$ could lead to complications, because it is possible for a particular realization of τ_x under $\mathbb{P}$ to have an infinite value, which could result in our code taking an infinite amount of time to run as it attempts to generate this realization. Therefore, we would like to obtain a new, *tilted* probability measure $\tilde{\mathbb{P}}$ under which Z_i is transformed into a new random variable $\tilde{Z}_i$ with negative drift; sampling from this measure will guarantee that $\tilde{\mathbb{P}}(\tau_x < \infty \mid X_0 = x) = 1$, ensuring that our code is able to run in finite time.

This technique is known as *importance sampling*, and our goal in subsequent sections of this report will be to implement it successfully.

6.3.3 Changing the Underlying Probability Measure via Exponential Tilting

Following the discussion in the previous section, we will now perform a change of measure which will enable us to perform importance sampling. Define the total change from the initial wealth, x, at the point where ruin is achieved to be

$$S_{\tau_x} = \sum_{i=1}^{\tau_x} Z_i. \tag{19}$$

It can be shown (although we do not provide the proof, since this is beyond the scope of ACT460) that there exists a distinct probability measure $\tilde{\mathbb{P}}$ and an optimal constant R^*, such that the following two facts hold true: (i) $\tilde{\mathbb{P}}$ is related to $\mathbb{P}$ through the *likelihood ratio*

$$\frac{d\tilde{\mathbb{P}}}{d\mathbb{P}} = \frac{e^{-R^* Z_i}}{M_{Z_i}(-R^*)} \tag{20}$$

where $M_{Z_i}(-R^*)$ is the moment-generating function of Z_i evaluated at $-R^*$, and (ii) $\tilde{Z}_i$, the distribution of Z_i under $\mathbb{P}$, has negative drift. Moreover, it can also be shown (we again omit the proof) that

$$\mathbb{P}(\tau_x < \infty | X_0 = x) = \mathbb{E}^{\tilde{\mathbb{P}}}[e^{R^* S_{\tau_x}}], \tag{21}$$

where the RHS of (21) denotes the expectation of $e^{R^* S_{\tau_x}}$ under $\tilde{\mathbb{P}}$. By (19) and (21), one can estimate $\psi_\infty(x)$ by first simulating a large number N_{sims} of realizations of $e^{R^* S_{\tau_x}}$ under $\tilde{\mathbb{P}}$, and then using the sample average as our estimate:

$$\widehat{\psi_\infty(x)}_{i.s.} = \frac{1}{N_{sims}} \sum_{j=1}^{N_{sims}} e^{R^* \tilde{S}_{\tau_x, j}} \tag{22}$$

where $\tilde{S}_{\tau_x, j}$ denotes the jth realization of S_{τ_x} under $\tilde{\mathbb{P}}$. However, in order to be able to compute this estimate, we must actually be able to correctly generate realizations of $\tilde{S}_{\tau_x, j}$. To do this, we will need to find $\tilde{Z}_i$, which is the distribution of Z_i under $\tilde{\mathbb{P}}$; once this is done, we will then be able to recover $\tilde{S}_{\tau_x, j}$ (which is just a sum of $\tilde{Z}_i$'s), and hence will be able to obtain the estimate in (22). Moreover, we will need to find the correct value of the optimal constant R^*.

6.3.4 Deriving the Adjustment Coefficient for Importance Sampling

The next step we take is to obtain the optimal constant R^* which was defined in the previous section. By [Gla03], R^* necessarily satisfies the constraint

$$\mathcal{K}_Y(R^*) + \log\left(\frac{\lambda}{\lambda + cR^*}\right) = 0, \tag{23}$$

where

$$\mathcal{K}_Y(t) = \log(M_Y(t)) = \log\left(\mathbb{E}[e^{tY}]\right) = \log\left(\frac{\alpha}{\alpha - t}\right) \tag{24}$$

is the cumulant generating function of the claim-size distribution. Furthermore, it is also required that $\mathcal{K}'_Y(R^*) > 0$; this ensures that $\tilde{\mathbb{P}}(\tau_x < \infty | X_0 = x) = 1$ [Gla03], and hence that sampling from $\tilde{\mathbb{P}}$ is guaranteed to be feasible.

Solving (23) with the parameters defined in Section 6.3.1, we find that $R^* = 0.5$.

6.3.5 Characterizing the Payout Process Under the Shifted Probability Measure

To find $\tilde{Z}_i$, the distribution of Z_i under $\tilde{\mathbb{P}}$, we will use the fact that if X and Y are two random variables, whose moment generating functions exist in an interval around 0 and satisfy $M_X(t) = M_Y(-t)$, then X has the same distribution as the negative of Y: $X \stackrel{d}{=} -Y$. Specifically, we claim that

$$M_{\tilde{Z}_i}(t) = M_{Z_i}(-t) = \frac{0.5}{(1-t)(0.5+t)}, \quad \text{for } t \in (-0.5, 0.5)\,, \tag{25}$$

given the parameters defined in Section 6.3.1 and the value of R^* derived in Section 6.3.4, and hence that $\tilde{Z}_i \stackrel{d}{=} -Z_i$. We prove our claim as follows.

By definition, $Z_i \stackrel{d}{=} c\xi_i - Y_i$. Notice that $c\xi_i$ and $-Y_i$ are independent, which implies that $M_{Z_i}(t) = M_{c\xi_i}(t)M_{-Y_i}(t)$. As $c\xi_i \sim c * Exponential(\lambda)$, we have that

$$M_{c\xi_i}(t) = \mathbb{E}^{\mathbb{P}}[e^{tc\xi_i}] = \int_0^\infty e^{tcx}\lambda e^{-\lambda x}dx = \frac{\lambda}{\lambda - ct}, \quad \text{for } t < \frac{\lambda}{c}. \tag{26}$$

Similarly, since $Y_i \sim Exponential(\alpha)$, we have

$$M_{-Y_i}(t) = \mathbb{E}^{\mathbb{P}}[e^{-Y_i t}] = \int_0^\infty e^{-ty}\alpha e^{-\alpha y}dy = \frac{\alpha}{\alpha + t}, \quad \text{for } t > -\alpha. \tag{27}$$

From this, we can see that

$$M_{Z_i}(t) = \frac{\lambda}{\lambda - ct}\frac{\alpha}{\alpha + t}, \quad \text{for } t \in \left(-\alpha, \frac{\lambda}{c}\right) \tag{28}$$

and hence, using the parameters set in Section 6.3.1, we get

$$M_{Z_i}(-t) = \frac{0.5}{0.5 + t}\frac{1}{1 - t} = \frac{0.5}{(1-t)(0.5+t)}, \quad \text{for } t \in (-1, 0.5) \tag{29}$$

as desired. It remains to show that $M_{\tilde{Z}_i}(t)$ is defined identically over some interval containing 0. Using the likelihood ratio defined in (20), we have that

$$M_{\tilde{Z}_i}(t) = \mathbb{E}^{\tilde{\mathbb{P}}}[e^{t\tilde{Z}_i}] = \mathbb{E}^{\mathbb{P}}\left[e^{tZ_i}\frac{d\tilde{\mathbb{P}}}{d\mathbb{P}}\right] = \frac{1}{M_{Z_i}(-R^*)}\mathbb{E}^{\mathbb{P}}[e^{(t-R*)Z_i}] = \frac{M_{Z_i}(t - R^*)}{M_{Z_i}(-R^*)}. \tag{30}$$

Using the definition of $M_{Z_i}(t)$ obtained in (28), the RHS of (30) becomes

$$M_{\tilde{Z}_i}(t) = \frac{\left(\frac{\lambda}{\lambda - c(t-R^*)}\right)\left(\frac{\alpha}{\alpha + (t-R^*)}\right)}{\left(\frac{\lambda}{\lambda + cR^*}\right)\left(\frac{\alpha}{\alpha - R^*}\right)} = \frac{(\lambda + cR^*)(\alpha - R^*)}{(\lambda - ct + cR^*)(\alpha + t - R^*)}. \tag{31}$$

With the parameters defined in Section 6.3.1, this becomes

$$M_{\tilde{Z}_i}(t) = \frac{(1)(0.5)}{(1-t)(0.5+t)} = \frac{0.5}{(1-t)(0.5+t)}, \quad \text{for } t \in (-0.5, 1). \tag{32}$$

Hence both $M_{\tilde{Z}_i}(t)$ and $M_{Z_i}(-t)$ are identical on the interval $(-0.5, 0.5)$, and the proof of our claim is complete. As such, we conclude that $\tilde{Z}_i \overset{d}{=} -Z_i$. The drift of $\tilde{Z}_i$ is then

$$-\mathbb{E}[Z_i] = -1 < 0, \tag{33}$$

and hence we have $\tilde{\mathbb{P}}(\tau_x < \infty | X_0 = x) = 1$ as desired. Thus, it is feasible to simulate realizations of (22), since $\tilde{S}_{\tau_x}$, the distribution of S_{τ_x} under $\tilde{\mathbb{P}}$, is guaranteed to take finite time to generate.

6.3.6 Simulating the Importance Sampling Estimator: Results and Discussion

Having obtained the distribution of $\tilde{Z}_i$, as well as the optimal constant R^*, we are now in a position to compute the estimate (22) in Python (our code for this part can be found in the Notebook). Setting $N_{sims} = 10000$ and using the parameters defined in Section 6.3.1, we obtain the result that

$$\widehat{\psi_\infty(x)}_{i.s.} = 2.26617 \times 10^{-5}. \tag{34}$$

It can be shown (though we omit the proof) that the analytical solution for the ultimate ruin probability of a Cramer-Lundberg wealth process is

$$\psi_\infty(x) = \frac{\lambda}{\alpha c} e^{-(\alpha - \frac{\lambda}{c})x} = 2.26999 \times 10^{-5}, \tag{35}$$

given that claim sizes are $Exponential(\alpha)$ [Emb97]. Comparing (34) with (35), we find that our estimate is extremely close to the true solution. This highlights the utility of importance sampling as a means of ultimate ruin probability estimation; in particular, we point out that under the original measure $\mathbb{P}$, we had $\mathbb{P}(\tau_x < \infty | X_0 = x) < 1$ due to the positive drift of Z_i, implying that sampling directly from $\mathbb{P}$ may have led to complications. By instead sampling from a new measure $\tilde{\mathbb{P}}$ where the event of ruin was guaranteed to occur (i.e., $\tilde{\mathbb{P}}(\tau_x < \infty | X_0 = x) = 1$), and then reweighting the probabilities accordingly, we were ultimately able to obtain a very accurate estimate of $\psi_\infty(x)$.

7 Conclusion

7.1 Summary of Results

In Section 2 of this report, we introduced a mathematical definition of the Cramer-Lundberg Model, and described its history, uses, and drawbacks. Uses of the model include ruin probability estimation, risk management, premium setting, and aggregate claims distributions. Drawbacks of the model include the fact that it does not account for the possibility of periodic premium payments, nor does it account for reserves or other cash flows as part of investment income. Further, it relies on numerous assumptions that may not be applicable in practice, such as the fact that claims amounts are independent and that extreme claim sizes are unlikely, which may not be the case in reality. Despite these shortfalls, the model is a historical baseline for the study of quantitative insurance risk management and inspired numerous models developed later in history which address said drawbacks.

In Section 4, we explored simulations of the Cramer-Lundberg using jump times and a fixed time grid. For the fixed time grid simulation of the model, we examined the impact of adjusting parameters on the resulting graphical results. We found that when k and θ were increased, a downwards trend in the wealth evolution was observed. For both parameters, the most highest values resulted in the most drastic downwards movement in the graphical results. When σ was increased, the numerical range of the final surplus of sample paths increased.

In Section 5, we simulated sample paths from an SDE approximation of the Cramer-Lundberg Model, and compared these sample paths to sample paths from the fixed time grid simulation implemented in Section 4. We found that the fixed time grid simulation provided much more jagged lines due to the discrete jumps arising from claims, while the SDE approximation was much smoother. Overall, the results from the simulations and the approximations differed significantly, however it was found that higher values the factor loading parameter (eta) resulted in much closer trends. Given large eta values, lambda and k values between two and five provided the most similar graphical results.

In Section 6, we computed Sample Mean and Control Variate estimators for ruin probabilities on a finite interval $[0, T]$ (where $T = 5$); these had values of 0.1512 and 0.1575. We also computed an importance sampling estimator for the ultimate ruin probability on $[0, \infty)$, assuming that the claim size Y was $Exponential(1)$; this had a value of 2.26617×10^{-5}.

7.2 Limitations & Next Steps

7.2.1 Fixed Time Grid Simulations: Limitations & Next Steps

The primary limitation of the fixed time grid simulations is that it does not include the Gaussian random variable G_i, which is used to introduce random noise in the model. It was excluded from the simulation to simplify the model and to focus analyzing the effect of a change in parameters, rather than to examine the additional random variations occurring at each time point. Although the simulation captures the Poisson process for claims and the gamma distribution fo claim sizes the effect of the exclusion of the Gaussian random variable could be further evaluated by reproducing the simulations following the provided algorithm in order to quantify the effect that these fluctuations may have on overall graphical trends, if any.

7.2.2 SDE Approximations: Limitations & Next Steps

For our simulations of the SDE Approximations in Section 5, we note that we did not simulate the sample paths of the fixed time grid exactly as per the algorithm we defined in Section 4.2, but instead opted to exclude the effect of the Gaussian random variable G_i at each time point. It is possible that this could have limited our ability to meet the requirements outlined in the project description, which specified that we were required to compare our implementation of this algorithm with the SDE approximation.

Accordingly, a next step for our work in Section 5 could be to simulate the fixed time grid algorithm exactly as described in Section 4,2, and compare our results with our simulations of the fixed time grid.

7.2.3 Limitations of Ruin Probability Estimation

While we devoted considerable effort towards ruin probability estimation in Section 6, it nevertheless remains true that the event of ruin rarely happens in practice, since insurance companies are unlikely to just sit and watch as their wealth dwindles to 0, and will instead take more proactive measures such as increasing the premium c in response to their financial difficulties, or diversifying their wealth across multiple portfolios so that ruin in one will not imply bankruptcy. As such, it is important to recognize that ruin probability is only a 'technical term', and that any estimate we obtain for it will likely not be reflective of the likelihood of such an event occurring in reality—especially when our estimates rely on simplified assumptions like those made by the Cramer-Lundberg model.

7.2.4 Next Steps for Ruin Probability Estimation

Since only one value was computed for each of the sample mean, control variate, and importance sampling estimators, there might be some variability which is present in our results. While we did attempt to capture this through tools such as variance calculations, next steps could be to simply calculate a larger number of estimates (i.e., around 100 or so) to gain further insights. Additionally, confidence intervals could be calculated for the sample mean and control variate estimators.

Another next step could be to experiment with varying the value of N_{sims}, in order to explore the relationship between this parameter and the values/variances of our estimates. Furthermore, we might wish to investigate whether implementing a control variate on the importance sampling estimator (22) could refine our estimate further, since we found that this was the case in Section 6.2.2.

References

[CT04] Rama Cont and Peter Tankov. *Financial Modelling with Jump Processes*. Chapman and Hall/CRC, 2004.

[Emb97] Paul Emberchts. "Risk Theory". In: (1997), p. 1. DOI: https://link.springer.com/chapter/10.1007/978-3-642-33483-2_2.

[Gla03] Paul Glasserman. *Monte Carlo Methods in Financial Engineering*. Springer, 2003.

[MB23] Michel Mandjes and Onno Boxma. *The Cramer-Lundberg Model and Its Variants*. Springer, 2023.

[Emb97] [CT04] [Gla03] [MB23]